# Optimal planetary landing with pointing and glide-slope constraints

Clara Leparoux[1,2], Bruno Hérissé[1] and Frédéric Jean[2]

***Abstract*— This paper studies a vertical powered descent problem in the context of planetary landing, considering glide-slope and thrust pointing constraints and minimizing any final cost. After stating the Max-Min-Max or Max-Singular-Max form of the optimal control deduced from the Pontryagin Maximum Principle, it theoretically analyzes the optimal trajectory for a more specific problem formulation to show that there can be at most one contact or boundary interval with the state constraint on each Max or Min arc.**

## I. Introduction

Interest for vertical landing problems has increased these recent years with the growing use of reusable launchers and as space exploration missions are requiring ever more landing precision. Vertical landing consists of two phases: first an entry phase, that set the vehicle in appropriate position and velocity conditions above the target to ensure landing feasibility, and then a phase of powered descent. Prior to the powered descent, the reference trajectory has to be recalculated in order to correct dispersions accumulated during the entry phase ([1]), or handle an update of the landing site. This motion planning problem is usually treated in an optimal control framework, allowing to minimize a quantity such as fuel consumption, flight time, or landing errors to ensure soft landing.

However, solving an optimal control problem efficiently and accurately remains a challenge ; moreover, analytical solutions, computed thanks to the Pontryagin Maximum Principle, are only known for simplified models with few constraints, as in [2] and [3]. This paper is concerned with the following dynamic model, expressed in an inertial frame $(e_x, e_y, e_z)$,

$$\begin{cases} \dot{r} &= v, \\ \dot{v} &= \frac{T}{m}u - g, \\ \dot{m} &= -q\|u\|, \end{cases} \tag{1}$$

where $r(t) = (x(t), y(t), z(t)) \in \mathbb{R}^3$ is the vehicle position, $v(t) \in \mathbb{R}^3$ is its velocity, $m(t) > 0$ is its mass, $q$ the maximal mass flow rate of the engine, $T > 0$ the maximal thrust and $g = (0, 0, g_0)$ with $g_0$ the gravitational acceleration. The thrust is controlled by the vector $u(t) \in \mathbb{R}^3$, where $||u|| \leq 1$ is the engine throttle. Previous theoretical and numerical studies tend to show that the structure of the optimal control for dynamics (1) generally consists of a finite succession of arcs on which the control norm is constant. Indeed, it is shown in [4] that the optimal control of the one dimension fuel-optimal problem with a bounded control follows an Off-Bang structure, i.e. it has a period of off thrust followed by full thrust until touchdown. Then, the Bang-Off-Bang structure, called Max-Min-Max when the thrust is not allowed to go to zero, has been found to be optimal for numerous variants of the problem, such as the two-dimensional problem studied in [5], the problem with specified initial and final thrust studied in [6], or with throttle and thrust angle control in [7]. Recently, [8] and [9] showed that the Max-Min-Max structure is the solution of the one dimension problem, minimizing the final time for the first one and considering the effect of an atmosphere on the thrust for the latter. However, there lack theoretical studies relating more complex formulations of the landing problem, for instance considering realistic technical and safety constraints. Among the existing numerical methods, a noteworthy one is presented in [2], [10], [11], that succeeds to solve efficiently the problem including constraints on the thrust direction and the launcher position, thanks to a convexification method. The simulations carried out in these studies also reveal a Max-Min-Max form of control.

In order to fill the gaps mentioned above, this paper analyzes a vertical landing problem which formulation considers relevant control and state constraints. We will consider, in addition to the bound on the control norm, a thrust pointing constraint limiting the amplitude of the control direction as well as the launcher orientation, both for safety reasons and to model actuator limitations. Then, we also take into account a glide-slope constraint, forcing the launcher position to stay inside a cone centered on the target, to ensure that the vehicle remains at a safe altitude and to guarantee sensor operability. The cost of the optimal control problem considered is expressed as a final cost, which embraces the most common applications such as maximizing the final mass or minimizing the final time. In this framework, we give elements to show that the optimal control has either a Max-Min-Max form or a Max-Singular-Max form. The complete proof on the structure of the optimal control is too long to be detailed here, but it is presented in [12]. Moreover, we analyze a particular case, in which the mass is assumed to be constant and the glide-slope constraint reduced to a positive altitude constraint. We show that in that configuration there are at most three contacts with the state constraint. Besides, we present numerical results that make us think that this outcome is likely to be generalized.

[1]Clara Leparoux (clara.leparoux@ensta-paris.fr) and Bruno Hérissé (bruno.herisse@onera.fr) are with DTIS, ONERA, Université Paris-Saclay, F-91123 Palaiseau, France.

[2] Clara Leparoux and Frédéric Jean (frederic.jean@ensta-paris.fr) are with UMA, ENSTA Paris, Institut Polytechnique de Paris, 91120 Palaiseau, France.

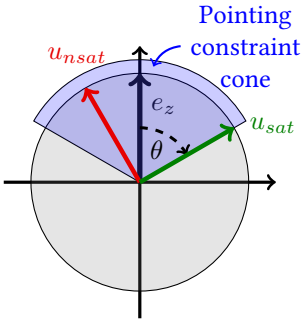


FIG. 1 – The thrust pointing constraint. Red : nonsaturating orientation. Green : saturating orientation.

This paper is organized as follows. In Section II, the full optimal control problem with constraints is presented, and the optimality conditions given by application of PMP are detailed. In Section III, the structure of the optimal control is stated and a sketch of proof is presented. Section IV studies a particular case of the landing problem to show that the number of contacts with the state constraint is limited. Finally, Section V provides numerical results.

## II. Problem statement

In this section, we state the optimal control problem and we detail the optimality conditions.

### A. Formulation

The study concerns vehicles having dynamics in the form of (1). The initial mass of the vehicle is denoted $m_0$ and its empty mass $m_e$. The state is denoted by $X = (r, v, m) \in \mathbb{R}^3 \times \mathbb{R}^3 \times \mathbb{R}$. We consider the following constraints :

- the fuel consumption is limited by the amount of fuel remaining in the vehicle :

$$m(t) > m_e \ \forall t \in [0, t_f);$$

- the thrust is limited, and it may not be possible to switch off the rocket engine during the powered descent. Thus, we impose upper and lower bounds on the control norm,

$$0 \leq u_{min} \leq \|u(t)\| \leq u_{max};$$

- the actuators performance for engine steering is limited and we would like to restrain the orientation of the rocket for physical and safety reasons. Thus, we add a pointing constraint (Fig.1) that forces the thrust direction to stay in a vertical cone of angle $\theta$, formulated as

$$\langle e_z, u \rangle \geq \|u\| \cos(\theta), \ \text{ with } \theta \in [0, \frac{\pi}{2});$$

- we want to prevent the vehicle from getting too close to the ground too early, since it would increase the risk to meet an obstacle and is not desirable for the operability of some sensors that require a good visibility of the landing site. Therefore, we add a glide-slope constraint (Fig.2), that constrains the vehicle position to stay inside a vertical cone of angle $\gamma$ taken from the horizontal,

$$h(r) = z - \tan(\gamma)\|(x, y)\| \geq 0, \ \text{ with } \gamma \in [0, \frac{\pi}{2}).$$

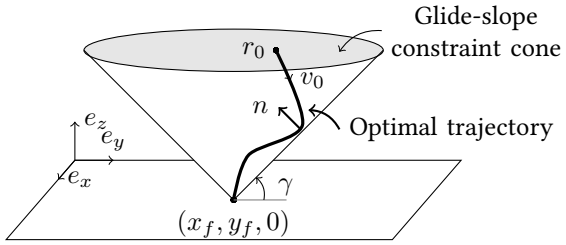


FIG. 2 – The glide-slope constraint.

A general formulation of the landing problem is chosen in order to cover the most common applications. The trajectory has to bring the vehicle from initial conditions $(r_0, v_0, m_0) \in \mathbb{R}^3 \times \mathbb{R}^3 \times \mathbb{R}$ to a target at null altitude and vertical velocity. Other final coordinates as well as the final time $t_f$ can be fixed or free. It minimizes a final cost, expressed in terms of the final time $t_f$ or the final state :

$$\min J := \ell(t_f, X(t_f)).$$

Thus, the complete optimal control problem can be written as follows

*Problem 1:*

$$\min \ell(t_f, X(t_f)) \text{ such that}$$

$$\begin{cases} (r(\cdot), v(\cdot), m(\cdot)) \in \mathbb{R}^3 \times \mathbb{R}^3 \times \mathbb{R} \text{ follows (1)}, \\ (r, v, m)(0) = (r_0, v_0, m_0)\,, \\ (z, v_z)(t_f) = (0, 0)\,, \\ m(t) > m_e \ \forall t \in [0, t_f), \\ u_{min} \leq ||u|| \leq u_{max}, \\ \langle e_z, u \rangle \geq \|u\| \cos(\theta), \\ h(r) \geq 0. \end{cases}$$

*Remark 2.1:* Note that one can not have $m(t) = m_e$ for some $t \in [0, t_f)$. Indeed it would imply that $u = 0$ on $[t, t_f]$, which makes impossible to reach $z(t_f) = 0$ with $v_z(t_f) = 0$. Thus, the mass constraint $m(t) > m_e$ plays no role in the problem.

### B. Optimality conditions

We give here the necessary optimality conditions provided by the application of the Pontryagin Maximum Principle to the optimal control Problem 1. Let us firstly specify some notations.

- For $p = (p_x, p_y, p_z) \in \mathbb{R}^3$, we set $\overline{p} = (p_x, p_y)$. Thus the glide-slope constraint writes as $h(r) = r_z - \tan(\gamma)\|\overline{r}\|$ and

$$n = \nabla h(r) = \begin{pmatrix} -\tan(\gamma)\frac{\overline{r}}{\|\overline{r}\|} \\ 1 \end{pmatrix}. \qquad (2)$$

– The control set is $\mathcal{U} = \{u \in \mathbb{R}^3 \ : \ u_{min} \leq \|u\| \leq u_{max}$ and $\langle e_z, u\rangle \geq \|u\|\cos(\theta)\}$.

We apply the version of the maximum principle given in [13, Th. 9.5.1], which in our case writes as follows. Define the Hamiltonian of Problem 1 as

$$H(X, P, u, p^0) = \langle p_r, v\rangle + \langle p_v, \frac{T}{m}u - g\rangle - p_m q\|u\|, \quad (3)$$

where the adjoint vector $P = (p_r, p_v, p_m)$ belongs to $\mathbb{R}^3 \times \mathbb{R}^3 \times \mathbb{R}$ and $p^0 \in \mathbb{R}$.

Let $(X(\cdot), u(\cdot))$ be an optimal solution of Problem 1. Then there exists a constant $p^0 = 0$ or $-1$, an absolutely continuous function $P(\cdot)$, and a nonnegative Borel measure $\mu$ on $[0, t_f]$, such that, writing

$$Q(t) = (q_r(t), p_v(t), p_m(t)), \quad (4)$$

$$q_r(t) = p_r(t) - \int_{[0,t)} n(s)\mu(ds), \quad (5)$$

we have :

1) $(P, p^0, \mu) \neq (0, 0, 0)$;
2) $\mathrm{supp}\{\mu\} \subset \{t \in [0, t_f] \ : \ h(r(t)) = 0\}$;
3) (dynamics of the adjoint vector) for a.e. $t \in [0, t_f]$,

$$\begin{cases} \dot{p}_r(t) &= 0, \\ \dot{p}_v(t) &= -q_r(t), \\ \dot{p}_m(t) &= \frac{T}{m(t)^2}\langle p_v(t), u(t)\rangle; \end{cases} \quad (6)$$

4) (maximization condition) for a.e. $t \in [0, t_f]$,

$$H(X(t), Q(t), p^0, u(t)) = \max_{w\in\mathcal{U}} H(X(t), Q(t), p^0, w); \quad (7)$$

5) (transversality condition)

$$\max_{w\in\mathcal{U}} H(X(t_f), Q(t_f), p^0, w) = -p^0\frac{\partial \ell}{\partial t}(t_f, X(t_f)). \quad (8)$$

## III. Solution of the optimal control problem

### A. Control structure

The main result of the paper gives the form of the optimal control of Problem 1.

*Theorem 1:* Consider an optimal trajectory on $[0, t_f]$. Then, the control $u(t)$ is in the Max-Min-Max or the Max-Singular-Max form, i.e. there exists $t_1$ and $t_2$ with $0 \leq t_1 \leq t_2 \leq t_f$ such that

$$\|u\|(t) = \begin{cases} u_{max} \text{ if } t \in [0, t_1) \cup (t_2, t_f], \\ u_{min} \text{ or singular if } t \in [t_1, t_2]. \end{cases}$$

*Remark 3.1:* When $t_1 = 0$ or $t_2 = t_f$, the Max-Min-Max or Max-Singular-Max form degenerates in a Max, Min, Singular, Max-Min, Max-Singular, Min-Max or Singular-Max form. Nevertheless, the result of subsection III-C specifies that the Max-Min-Max form and its degenerate variations prevail.

### B. Sketch of proof

The complete proof of Theorem 1 is too long and technical to be presented in this paper; it is detailed in [12]. Here we report the main steps we went through to achieve it.

First, we deduce from the maximization condition (7) the expression of the optimal control, provided in Lemma 2.

*Lemma 2:* Let $u(t)$, $t \in [0, t_f]$, be an optimal control of Problem 1, and $P = (p_r, p_v, p_m) \in \mathbb{R}^3 \times \mathbb{R}^3 \times \mathbb{R}$ its adjoint vector. Then, for any $t \in [0, t_f]$ such that $u(t) \neq 0$, there holds

$$\frac{u(t)}{\|u(t)\|} = d(t),$$

where $d : [0, t_f] \to \mathcal{S}^2$ is a measurable function satisfying $d(t) =$

$$\begin{cases} \frac{p_v(t)}{\|p_v(t)\|} \\ \qquad \text{if } p_{v_z}(t) \geq \|p_v(t)\|\cos(\theta) \text{ and } p_v(t) \neq 0, \\ \left(\sin(\theta)\frac{\overline{p}_v(t)}{\|\overline{p}_v(t)\|}, \cos(\theta)\right) \\ \qquad \text{if } p_{v_z}(t) < \|p_v(t)\|\cos(\theta) \text{ and } \overline{p}_v(t) \neq 0, \\ \left(\sin(\theta)\delta, \cos(\theta)\right) \text{ with } \delta \in \mathcal{S}^1 \\ \qquad \text{if } p_{v_z}(t) < \|p_v(t)\|\cos(\theta) \text{ and } \overline{p}_v(t) = 0. \end{cases} \quad (9)$$

Moreover, set

$$\Psi(t) = \frac{T}{m}\langle p_v(t), d(t)\rangle - p_m(t)q. \quad (10)$$

Then,

$$\|u(t)\| = \begin{cases} u_{max} & \text{if } \Psi(t) > 0, \\ u_{min} & \text{if } \Psi(t) < 0. \end{cases}$$

Hence, the optimal control consists of arcs on which its norm is either saturated to its minimal or maximal bound, except if $\Psi$ is zero then the control is singular. The purpose of the proof is to show that the sign of $\Psi$ changes at most two times, or remains zero on a single interval, and is positive out of this interval. This amounts to show that $\Psi$ crosses zero at most two times, which can be done by studying the variations of $\Psi$ since we can prove that $\Psi$ is absolutely continuous.

The variations of $\Psi$ are obtained from the sign of its derivative, which is the opposite of the one of $\langle q_r, d\rangle$. The study of $\langle q_r, d\rangle$ poses the following difficulties. First, working with $d$ requires to treat differently the intervals on which the pointing constraint is active or not, since its expression is not the same. Furthermore, $d$ is not absolutely continuous in general and it is undefined when $p_v$ is zero or when $\overline{p}_v$ is zero and $p_{v_z}$ is negative; thus, the intervals on which this can happen have to be treated separately. Finally, $q_r$ is defined by (5) and might have discontinuities when the states constraint is activated. This implies that $\langle q_r, d\rangle$ is not differentiable when the state constraint is active. Consequently, to go to the conclusion, it is necessary to show in the first hand that the derivative of $\langle q_r, d\rangle$ is negative where it exists, and on the other hand that

the discontinuities of $\langle q_r, d\rangle$ do not cause additional sign changes (see [12]).

### C. Singular arcs in the case of an altitude constraint

Despite the fact that Theorem 1 does not exclude the existence of singular trajectories, it seems that they do not appear in general. They seldom arise when solving landing problems numerically, and the next lemma states that they do not exist in the case of an altitude constraint ($\gamma = 0$) if the initial conditions are generic, which is defined in Lemma 3. The result of Lemma 3 has been proved in [12] under the two following assumptions.

*Assumption 1:* We put ourselves in the context of an altitude constraint, setting $\gamma = 0$. In that case, $n = e_z$, so $\overline{q}_r = \overline{p}_r$ is constant even when $h(r) = 0$.

*Assumption 2:* We assume that the final position and velocity are fixed and null, i.e. $r(t_f) = r_f = 0$ and $v(t_f) = v_f = 0$.

*Lemma 3:* If the optimal trajectory contains a singular arc, then the initial conditions are such that $(x, y)(0)$ and $(v_x, v_y)(0)$ are collinear. Consequently, for generic initial conditions there are no singular arcs in the optimal trajectories.

Lemma 3 helps to explain why singular trajectories seem to be rare and are often dismissed in the literature. Assumptions have been made here in order to give a simple proof but they could probably be extended, for example by continuity arguments. Particularly, the assumption that initial conditions are generic mainly spreads out problems in two dimensions, but it is clear that even in that case singular trajectories are not frequent, and they did not appear in numerical results of Section V.

## IV. Number of contacts with the altitude constraint

We study now a particular case of Problem 1 in order to show that optimal trajectories meet the state constraint only a very limited number of times. More precisely, Corollary 5 states that in the conditions of Lemma 3 there can be at most two contacts before reaching the final point. To complete the proof, we made the assumption that the mass $m$ is constant (i.e. $q = 0$), and we assume that the state constraint is an altitude constraint as in Assumption 1. Let us start with some definitions. Given a trajectory, we say that $[t_{c_1}, t_{c_2}]$ is a *boundary interval* if $h(t) = 0$ for all $t \in [t_{c_1}, t_{c_2}]$, and $[t_{c_1}, t_{c_2}]$ is the largest interval satisfying this condition and containing $t_{c_1}, t_{c_2}$. When the boundary interval is reduced to a point $t_c$ (i.e. $t_{c_1} = t_{c_2} = t_c$), we rather say that $t_c$ is a *contact point.*

*Lemma 4:* There is at most one contact point or boundary interval on each Max or Min arc.

*Proof:*

Let us show that there is at most one contact point or boundary interval on each Max arc (including possibly the final point for the last Max arc). A similar reasoning on Min arcs will then give the conclusion. By contradiction, assume that the same Max arc contains two different boundary intervals $[t'_{c_1}, t_{c_1}]$ and $[t_{c_2}, t'_{c_2}]$, with $t_{c_1} < t_{c_2}$. We can moreover assume that $h(t) = z(t) > 0$ on $(t_{c_1}, t_{c_2})$. Then

$$\dot{v}_z(t_{c_1}) \geq 0, \quad \dot{v}_z(t_{c_2}) \geq 0, \tag{11}$$

and there exists $t_b \in (t_{c_1}, t_{c_2})$ such that $\dot{v}_z(t_b) < 0$.

Note that $\dot{v}_z$ is an affine function of $d_z$, the vertical component of $d$,

$$\dot{v}_z = u_{max}\frac{T}{m}d_z - g_0,$$

so the above sign condition on $\dot{v}_z$ writes as

$$d_z(t_{c_1}) \text{ and } d_z(t_{c_2}) \geq \frac{mg_0}{Tu_{max}}, \qquad d_z(t_b) < \frac{mg_0}{Tu_{max}}. \tag{12}$$

Now, on $(t_{c_1}, t_{c_2})$, the state constraint is inactive, therefore $q_r = q_r(t_{c_1})$ is constant and

$$p_v(t) = p_0 - q_r t, \quad \forall t \in (t_{c_1}, t_{c_2}).$$

Assume first that $p_0$ and $q_r$ are collinear, and write $p_0 = \rho_0\delta$ and $q_r = \rho_r\delta$, with $\rho_0, \rho_r \in \mathbb{R}$ and $\delta \in \mathcal{S}^2$. Thus,

$$\frac{p_v}{\|p_v\|} = \text{sign}(\rho_0 - \rho_r t)\delta.$$

We deduce that $d_z$ can take only two values, $\cos(\theta)$ and the constant value $|\delta_z|$ (if this value belongs to $(\cos(\theta), 1]$), and can change value at most one time. This contradicts (12).

Thus $p_0$ and $q_r$ are not collinear. In particular $d$ is absolutely continuous on $(t_{c_1}, t_{c_2})$. First, let us notice that when the pointing constraint is active, $d_z$ is constantly equal to $\cos(\theta)$, and study now the evolution of $d_z$ when the pointing constraint is not active. We will reduce the problem to two dimensions. Let us choose $\hat{n} = \pm\frac{p_0 \wedge q_r}{\|p_0 \wedge q_r\|}$ such that $\langle \hat{n}, e_z\rangle \geq 0$. Then $d$, which is equal to $\frac{p_v}{\|p_v\|}$, belongs to the normal plane to $\hat{n}$, denoted $\hat{n}^\perp$. Note that $\hat{n} \neq e_z$. Indeed, otherwise $p_{v_z} = 0$, which implies that $d_z$ is constantly equal to $\cos(\theta)$ and is in contradiction with (12). Let $\alpha$ be the angle between $\hat{n}$ and the plane $(e_x, e_y)$ and let us choose $(u_1, u_2)$ an orthonormal basis of $\hat{n}^\perp$ such that $\langle u_1, e_z\rangle = 0$ and $\langle u_2, e_z\rangle = \cos(\alpha) > 0$. Then, we define $\phi$ such that $d$ can be written

$$d = \cos(\phi)u_1 + \sin(\phi)u_2$$

with $\phi \in [-\frac{\pi}{2}, \frac{\pi}{2}]$ and we have that

$$d_z = \sin(\phi)\cos(\alpha).$$

We have from (12) that $\phi(t_{c_1})$ and $\phi(t_{c_2})$ are in $(0, \frac{\pi}{2})$. Now, let us show that the evolution of $d_z$ contradicts (12). Since $\alpha$ is constant,

$$\dot{d}_z = \dot{\phi}\cos(\phi)\cos(\alpha), \tag{13}$$

therefore, $\dot{d}_z$ has the same sign as $\dot{\phi}$, and $\dot{\phi}$ can be expressed thanks to the following computations. We reduce ourselves to $\hat{n}^\perp$, since $p_v$, $p_0$ and $q_r$ belongs to it. We place ourselves in this plane in the coordinates defined by $(u_1, u_2)$. By abuse of notation, we will call $p_v$ the vector in two dimensions defined by $p_v = (\langle p_v, u_1\rangle, \langle p_v, u_2\rangle)$. As

$p_v = \|p_v\| d = \|p_v\| \begin{pmatrix} \cos(\phi) \\ \sin(\phi) \end{pmatrix}$, then

$$\dot{p}_v = \frac{d\|p_v\|}{dt} \begin{pmatrix} \cos(\phi) \\ \sin(\phi) \end{pmatrix} + \|p_v\| \dot{\phi} \begin{pmatrix} -\sin(\phi) \\ \cos(\phi) \end{pmatrix},$$

and by multiplying on the left by $\begin{pmatrix} -\sin(\phi) & \cos(\phi) \end{pmatrix}$ we obtain

$$\begin{pmatrix} -\sin(\phi) \\ \cos(\phi) \end{pmatrix}^\top (-q_r) = \|p_v\| \dot{\phi}.$$

We deduce that

$$\dot{\phi} = -\frac{1}{\|p_v\|^2} \det(q_r, p_v) = -\frac{1}{\|p_v\|^2} \det(q_r, p_0).$$

As $q_r$ and $p_0$ are constant, we deduce that $\dot{\phi}$ is of constant sign, and $\dot{d}_z$ also from (13). Thus, $d_z$ is monotonous when the pointing constraint is not active and constant when it is active: we conclude that it is not possible to verify (12). ■

Adding Assumption 2 to ensure that the optimal control is Max-Min-Max, the next result is deduced from Lemma 4.

*Corollary 5:* Under assumptions 1 and 2 and for generic initial conditions, there are at most three contact points or boundary intervals along the trajectory. More precisely,

1) if $u_{min} < \frac{m_0 g_0}{T}$, there is along the trajectory at most two contact points or boundary intervals ;
2) if $u_{min} \cos(\theta) \geq \frac{m_0 g_0}{T}$, the only possible contact point is the final point.

*Proof:* The main statement follows by application of Theorem 1 and Lemma 3, which implies that the control is of the form Max-Min-Max (or the restriction of such a control to a subinterval), and Lemma 4 gives us the number of contacts. Then, the assumption of Point 1 implies that $u_{min} T$ does not compensate the weight of the vehicle, therefore it is not possible to have a contact on a Min arc without violating the state constraint. Finally, the assumption of Point 2 implies that $u(t)T$ compensate the weight of the vehicle for any control direction, therefore the vertical velocity, and so the altitude, would remain positive after a contact with the state constraint. We deduce that it is not possible to have a contact aside from the final point. ■

*Remark 4.1:* The last result has been demonstrated with the assumption of a constant mass. However we expect that it still holds if the mass has small variations, i.e. $q$ is small. Indeed, the reasoning is still correct if $m(t_b) \sim m(t_{c_1})$ or $m(t_{c_2})$, therefore it is sufficient to assume that the mass varies only slightly between two contact points. Likewise, the same reasoning would work with a glide-slope constraint of $\gamma \neq 0$, by assuming that $n$ is constant, which means in 2 dimensions that the trajectory stays in the same half-plane $x \geq 0$ or $x \leq 0$.

## V. Numerical results

This section presents some examples for a Mars powered descent problem, in two dimensions for the sake of simplicity. We present examples covering different situations that may or may not fall within the scope of the results of section IV in order to highlight that the numerical solutions vary little and thus justify that the results of the paper could surely be extended in a larger framework. The simulations are carried out by using CasADi ([14]) with python language and the IPOPT solver. They are performed under the same conditions as in [2]. The launcher parameters are $T = 16573N$, $u_{min} = 0.3$, $u_{max} = 0.8$ and $m_e = 1505kg$, and $g_0 = 3.71m/s^2$ corresponds to the Mars gravitational acceleration. The initial state is given by $r_0 = [2000, 1500]m$, $v_0 = [100, -75]m/s$ and $m_0 = 1905kg$, and the final time $t_f$ is free. The optimal control problem considered will aim to perform a pinpoint landing by steering the vehicle to null final position and velocity.

The first set of simulations is performed in the conditions of section IV with a vehicle mass constant, i.e. with $q = 0$. In the usual way, we would minimize fuel consumption, as in the next example, with a cost proportional to

$$J = \int_0^{t_f} \|u\| dt.$$

Here, we minimize this cost to obtain the solution of an equivalent problem. It is straightforward to show that all results presented in Section III and IV remain valid under these conditions. Note that the assumption of the Point 1 of Corollary 5 $u_{min} < \frac{m_0 g_0}{T}$ is verified.

Three simulations were performed using the conditions described above. The first executes a Mars landing if no pointing and altitude constraint is applied. Fig.3 shows that in that case, the zero altitude is crossed. In the second simulation, an altitude constraint has been added. We see that, in accordance with the results of Corollary 5, there are two contact points with the state constraint along the trajectory : one during the first Bang arc and the final point. Finally, in the third example, a pointing constraint of $45°$ is added. There are again two contacts with the state constraints, and the pointing constraint is active during the last $16s$ of the trajectory, which has the effect of making the trajectory more vertical.

A second set of simulations has been performed with a varying mass, with $q = 8.4294kg/s$, considering a glide-slope constraint of $\gamma = 5°$ and maximizing the final mass of the vehicle :

$$J = -m(t_f) = -m(0) + \int_0^{t_f} q\|u\| dt.$$

In that case, the constraints are more compelling, as we see on the green plot on Fig.4 that the thrust direction is saturated by the pointing constraint on both its inferior and its superior bounds. There is still one contact point

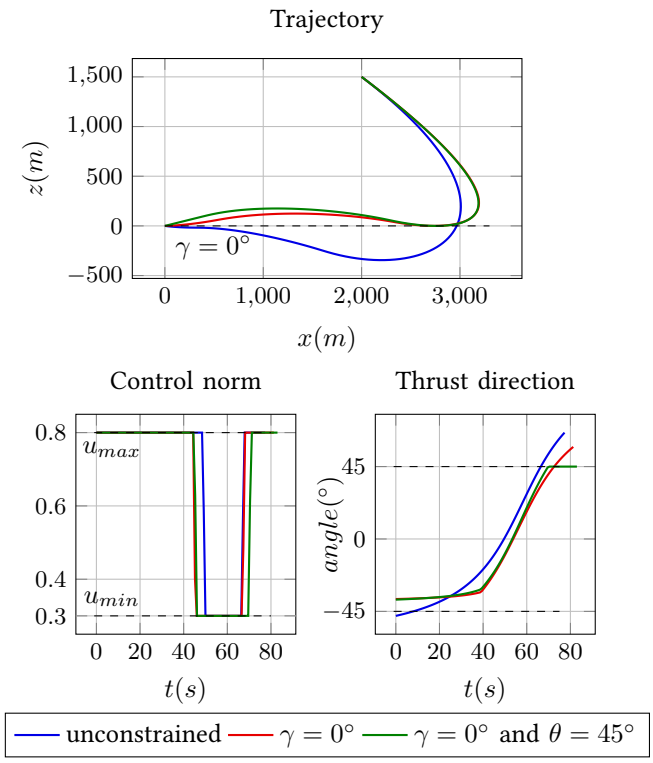


FIG. 3 – Simulation results for $q = 0$ without glide-slope or pointing constraint (blue), with only a glide-slope constraint of $\gamma = 0°$ (red) and with glide-slope and pointing constraints for $\theta = 45°$ (green).

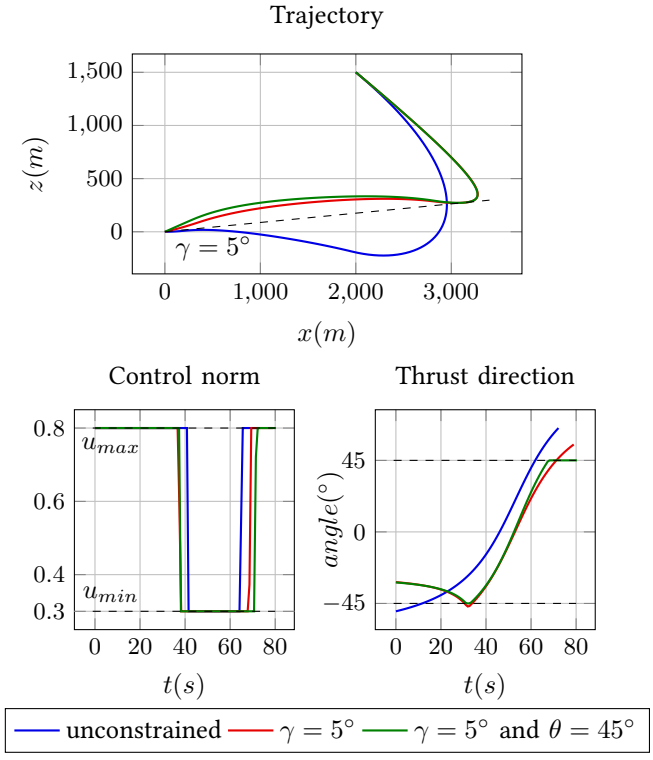


FIG. 4 – Simulation results with a varying mass, and a glide-slope constraint of $\gamma = 5°$.

with the state constraint, although we leave the framework of Corollary 5. Remark that in all examples the form of the control is Max-Min-Max, and even the switching times vary little from one simulation to another.

## VI. Conclusion and Perspectives

We showed that the optimal control of the powered descent problem with glide-slope and pointing constraints is Max-Min-Max for generic initial conditions. The analytical study of the constant mass problem also proved that there can be at most one contact with the state constraint on each Max or Min arc. These results are verified in numerical simulations. Thus, the theoretical and numerical results highlight the rigidity of the structure of the solution of powered descent problems, since it is identical for different cost functions and changes slightly when adding control and state constraints, which suggests that it is not specific to the problem formulation. Moreover, we can extend the result of Theorem 1 for a problem formulation without the glide-slope and pointing constraints but taking into account the effect on the thrust of a constant pressure, which is a fine modelling of planetary atmosphere at low altitude. The results of [9] let us think that it is also valuable for a varying pressure, and the proof is left as a subject of future work.

## References


[1] L. Blackmore, "Autonomous precision landing of space rockets," *The Bridge*, vol. 46, no. 4, pp. 15–20, 2016.

[2] B. Acikmese and S. Ploen, "Convex programming approach to powered descent guidance for mars landing," *Journal of Guidance, Control, and Dynamics*, vol. 30, pp. 1353–1366, sep 2007.

[3] P. Lu, "Propellant-optimal powered descent guidance," *Journal of Guidance, Control, and Dynamics*, vol. 41, no. 4, pp. 813–826, 2018.

[4] J. Meditch, "On the problem of optimal thrust programming for a lunar soft landing," *IEEE Transactions on Automatic Control*, vol. 9, pp. 477–484, oct 1964.

[5] G. Leitmann, "On a class of variational problems in rocket flight," *Journal of the Aerospace Sciences*, vol. 26, pp. 586–591, sep 1959.

[6] U. Topcu, J. Casoliva, and K. Mease, "Fuel efficient powered descent guidance for mars landing," in *AIAA Guidance, Navigation, and Control Conference and Exhibit*, American Institute of Aeronautics and Astronautics, jun 2005.

[7] U. Topcu, J. Casoliva, and K. Mease, "Minimum-fuel powered descent for mars pinpoint landing," *Journal of Spacecraft and Rockets*, vol. 44, pp. 324–331, mar 2007.

[8] F. Gazzola and E. M. Marchini, "A minimal time optimal control for a drone landing problem," *ESAIM : COCV*, vol. 27, p. 99, 2021.

[9] H. Ménou, E. Bourgeois, and N. Petit, "Fuel-optimal program for atmospheric vertical powered landing," in *2021 60th IEEE Conference on Decision and Control (CDC)*, pp. 6312–6319, 2021.

[10] L. Blackmore, B. Açikmeşe, and D. P. Scharf, "Minimum-landing-error powered-descent guidance for mars landing using convex optimization," *Journal of guidance, control, and dynamics*, vol. 33, no. 4, pp. 1161–1171, 2010.

[11] B. Acikmese, J. Carson, and L. Blackmore, "Lossless convexification of the soft landing optimal control problem with non-convex control bound and pointing constraints," *IEEE Transactions on Control Systems Technology*, vol. 21, no. 6, pp. 2104–2113, 2013.

[12] C. Leparoux, B. Hérissé, and F. Jean, "Structure of optimal control for planetary landing with control and state constraints." ArXiv preprint arXiv:2204.06794, 2022.

[13] R. Vinter, *Optimal Control*. Birkhäuser, jul 2010.

[14] J. A. E. Andersson, J. Gillis, G. Horn, J. B. Rawlings, and M. Diehl, "CasADi – A software framework for nonlinear optimization and optimal control," *Mathematical Programming Computation*, vol. 11, no. 1, pp. 1–36, 2019.